J Appl Electrochem (2010) 40:543–549
DOI 10.1007/s10800-009-0026-9

ORIGINAL PAPER

Thermodynamics of chromate replacements by various homologous transition metal oxyanions

E. McCafferty

Received: 22 June 2009 / Accepted: 25 September 2009 / Published online: 10 October 2009

Abstract The free energy change is calculated for the interaction of 19 different oxyanions (metalates) with iron (steel) or aluminum surfaces. The oxyanions considered here are those of the transition metals in the fourth through sixth periods of the periodic table. The oxyanions which produce more negative values of ΔG^{o} (per mole of oxyanion) than that of chromate (CrO_4^{-2}) are permanganate (MnO_4^{-}), nickelate (NiO_4^{-2}), ruthenate (RuO_4^{-} or RuO_4^{-2}), and rhodate (RhO_4^{-2}). The oxyanions which produce values of ΔG^{o} (per mole of oxyanion) similar to CrO_4^{-2} are osmate (OsO_4^{-2}), and iridate (IrO_4^{-2}).

Keywords Chromate replacements · Oxyanions · Metalates · Thermodyamics · Corrosion

1 Introduction

Chromates are effective corrosion inhibitors when added to aqueous solutions and are also useful as conversion coatings. That is, surface treatment of a metal with chromates produces a mixed oxide of Cr_2O_3 and the oxide of the underlying substrate. In the past, chromates have been used to treat surfaces of steel, aluminum, and galvanized steel.

However, it is now widely understood that the use of chromates presents health and environmental problems due to the toxicity of the Cr^{+6} species and due to the persistence of the chromate ion, as evidenced by its intense yellow color [1, 2].

Thus, there is an ongoing effort to identify effective chromate replacements. One approach is to use analogous oxyanions of transition metals other than chromium. Experimental studies have been done on the use of molybdates [3–7], vanadates [3, 8], tungstates [3, 4, 6], and permanganate [9]. Other related approaches have involved the use of cerium salts [10], phosphates [11], hydrotalcite inorganic coatings [12], the addition of non-chromates to organic coatings [13], and the use of alkoxy-titanates [14, 15] or alkoxy-zirconates [15].

The purpose of this communication is to consider the thermodynamics of various oxyanions of transition metals in their interaction with iron (steel) or aluminum surfaces. The oxyanions considered here are those of the transition metals shown in Fig. 1, which is a portion of the periodic table. Appropriate thermodynamic data are available (or can be estimated) for the elements which are shaded gray in Fig. 1.

The oxyanions considered here are titanate ($HTiO_3^{-}$), vanadate (VO_4^{-3}), chromate (CrO_4^{-2}), permanganate (MnO_4^{-}), nickelate (NiO_4^{-2}), zirconate ($HZrO_3^{-}$), niobate (NbO_3^{-}), molybdate (MoO_4^{-2}), pertechnetate (TcO_4^{-}), ruthenate (RuO_4^{-2} and RuO_4^{-}), rhodate (RhO_4^{-2}), hafnate (HfO_3^{-2}), tantalate (TaO_3^{-}), tungstate (WO_4^{-2}), rhenate (ReO_4^{-2} and ReO_4^{-}), osmate (OsO_4^{-2}), and iridate (IrO_4^{-2}).

These thermodynamic calculations are intended to assist further experimental studies. Oxide films which form under thermodynamically spontaneous conditions are candidates for further studies involving reaction kinetics, surface analysis, the use of oxyanion surface treatments prior to the application of organic coatings, and long-term corrosion testing and evaluation.

E. McCafferty (✉)
Science Applications International Corporation, Naval Research Laboratory, Washington, DC 20375, USA
e-mail: mccafferty@anvil.nrl.navy.mil

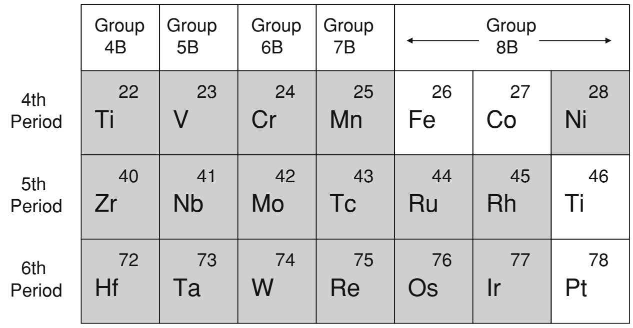

	Group 4B	Group 5B	Group 6B	Group 7B	← Group 8B →		
4th Period	22 Ti	23 V	24 Cr	25 Mn	26 Fe	27 Co	28 Ni
5th Period	40 Zr	41 Nb	42 Mo	43 Tc	44 Ru	45 Rh	46 Ti
6th Period	72 Hf	73 Ta	74 W	75 Re	76 Os	77 Ir	78 Pt

Fig. 1 A portion of the periodic table showing metallic elements for which oxyanions were considered as chromate replacements. Atomic numbers are given for each element shown. Thermodynamic data are available or can be estimated for the elements shaded gray in the figure

2 Thermodynamic calculations and results

2.1 Cathodic half-cell reactions

Half-cell cathodic reactions for several familiar oxyanions and the corresponding expressions for the cathodic electrode potential are given in Table 1, and are taken from Pourbaix's Atlas [16]. The form of the resulting oxide in each half-cell reaction is based on the oxide stability according to the Pourbaix diagram [16] or is taken from available surface analysis by X-ray photoelectron spectroscopy (XPS) [9, 17–25]. The reduction of tungstate (WO_4^{-2}) was considered to form either WO_2 or W_2O_5.

Calculations for each of the oxyanions listed in Table 1 were performed for pH 0, 7, and 14 and for oxyanion concentrations ranging from 1×10^{-6} to 1 M. Figure 2 shows calculated results for pH 7.

Figures 3 and 4 show results for pH 0 and pH 14, respectively. It can be seen that the calculated half-cell reduction potential depends markedly on the pH and also on the concentration of the oxyanion.

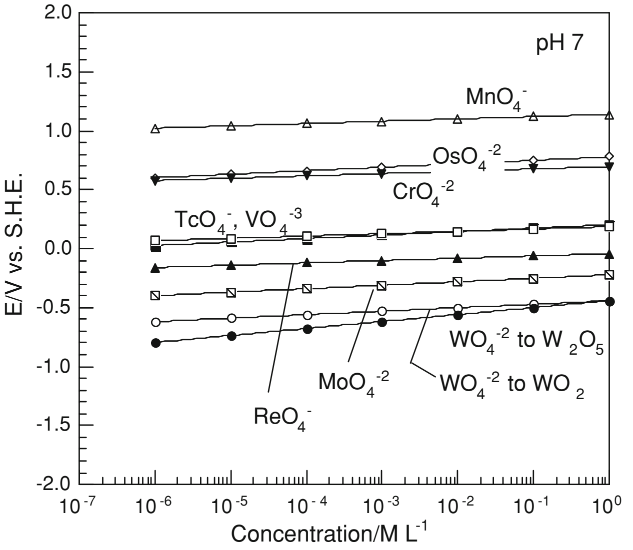

Fig. 2 Results of calculations for the formation of oxides by the electrochemical reduction of various oxyanions at pH 7

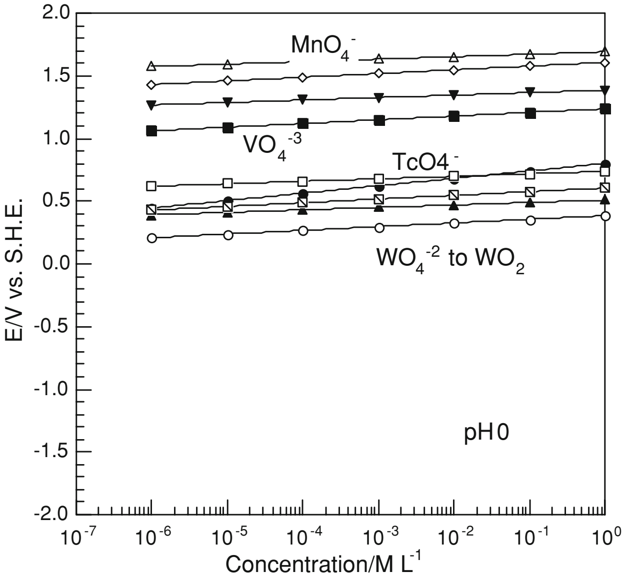

Fig. 3 Results of calculations for the formation of oxides by the electrochemical reduction of various oxyanions at pH 0

Table 1 Reduction reactions of various oxanions of transition metals and the reduction potential

$MnO_4^- + 4H^+ + 3e^- \rightarrow MnO_2 + 2H_2O$	$E = 1.692 - 0.0788\ pH + 0.0197 \log [MnO_4^-]$
$TcO_4^- + 4H^+ + 3e^- \rightarrow TcO_2 + 2H_2O$	$E = 0.738 - 0.0788\ pH + 0.0197 \log [TcO_4^-]$
$ReO_4^- + 4H^+ + 3e^- \rightarrow ReO_2 + 2H_2O$	$E = 0.510 - 0.0788\ pH + 0.0197 \log [ReO_4^-]$
$2CrO_4^{-2} + 10H^+ + 6e^- \rightarrow Cr_2O_3 + 5H_2O$	$E = 1.386 - 0.0985\ pH + 0.0197 \log [CrO_4^{-2}]$
$MoO_4^{-2} + 4H^+ + 2e^- \rightarrow MoO_2 + 2H_2O$	$E = 0.606 - 0.1182\ pH + 0.0295 \log [MoO_4^{-2}]$
$OsO_4^{-2} + 4H^+ + 2e^- \rightarrow OsO_2 + 2H_2O$	$E = 1.607 - 0.1182\ pH + 0.0295 \log [OsO_4^{-2}]$
$WO_4^{-2} + 4H^+ + 2e^- \rightarrow WO_2 + 2H_2O$	$E = 0.386 - 0.1182\ pH + 0.0295 \log [WO_4^{-2}]$
$2WO_4^{-2} + 6H^+ + 2e^- \rightarrow W_2O_5 + 3H_2O$	$E = 0.801 - 0.1773\ pH + 0.0591 \log [WO_4^{-2}]$
$2VO_4^{-3} + 10H^+ + 4e^- \rightarrow V_2O_3 + 5H_2O$	$E = 1.238 - 0.1477\ pH + 0.0295 \log [WO_4^{-2}]$

2.2 Overall reactions with iron

The section above pertains to the cathodic half-cell reaction alone, but the anodic half-cell reaction also must be

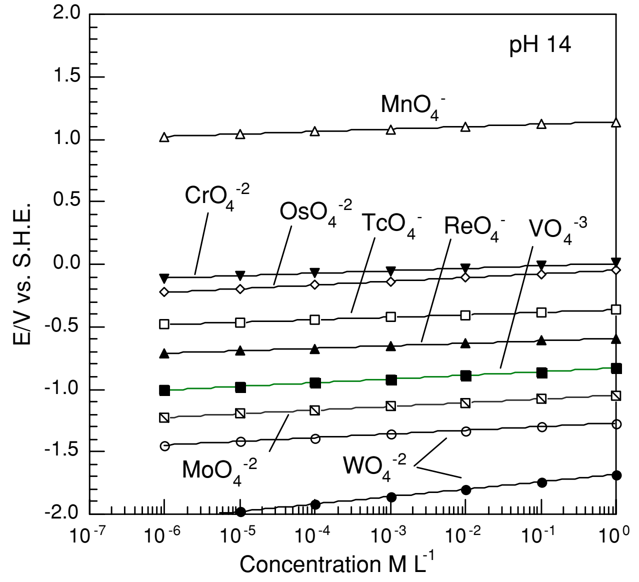

Fig. 4 Results of calculations for the formation of oxides by the electrochemical reduction of various oxyanions at pH 14

considered. In the interaction of molybdate inhibitors with iron, for example, the cathodic half-cell reaction is:

$$MoO_4^{-2} + 4H^+ + 2e^- \rightarrow MoO_2 + 2H_2O \quad (1)$$

and the anodic reaction is:

$$2Fe + 3H_2O \rightarrow Fe_2O_3 + 6H^+ + 6e^-. \quad (2)$$

The overall reaction is the sum of these two half-cell reactions:

$$2Fe + 3MoO_4^{-2} + 6H^+ \rightarrow Fe_2O_3 + 3MoO_2 + 3H_2O. \quad (3)$$

The standard free energy change for the overall reaction is given by:

$$\Delta G^o = \sum_i v_i \mu_i^o(\text{products}) - \sum_i v_i \mu_i^o(\text{reactants}). \quad (4)$$

where v_i are the stoichiometric coefficients and μ_i^o are the chemical potentials (also called partial molar free energies of formation ΔG_f^o) of the various species in their standard states. For this example,

$$\Delta G^o = [\mu^o(Fe_2O_3) + 3\mu^o(MoO_2) + 3\mu^o(H_2O)] - \left[2\mu^o(Fe) + 3\mu^o\left(MoO_4^{-2}\right) + 6\mu^o(H^+)\right] \quad (5)$$

where $\mu^o(Fe) = 0$ and $\mu^o(H^+) = 0$. Values of μ^o for the other chemical species in Eq. 5 were taken from Pourbaix's Atlas [16]. The result is: $\Delta G^o = -380$ kJ. Normalized per mole of inhibitor, $\Delta G^o = -380$ kJ per 3 moles MoO_4^{-2}, or -127 kJ mole^{-1} MoO_4^{-2}.

Similar calculations were performed for oxyanion species of various transition elements, as shown in Table 2. Values of μ_i^o were taken from Pourbaix [16] or Bard [26]. Values for $\mu^o(HfO_3^{-2})$ and $\mu^o(TaO_3^-)$ are not available but were estimated as follows. For the oxyanions where data are available, a plot of μ^o versus the radius of the central cation in the oxyanion gave a linear plot, from which $\mu^o(HfO_3^{-2})$ and $\mu^o(TaO_3^-)$ were calculated (Fig. 5). The calculated results are: $\mu^o(HfO_3^{-2}) = -1{,}169$ kJ mole^{-1}

Table 2 Overall reactions of various transition metal oxyanions with an iron surface

Oxyanions of transition metals of the fourth period
$HTiO_3^- + H^+ \rightarrow TiO_2 + H_2O$
$6VO_4^{-3} + 4Fe + 18H^+ \rightarrow 3V_2O_3 + 2Fe_2O_3 + 9H_2O$
$2CrO_4^{-2} + 2Fe + 4H^+ \rightarrow Cr_2O_3 + Fe_2O_3 + 2H_2O$
$2MnO_4^- + 2Fe + 2H^+ \rightarrow 2MnO_2 + Fe_2O_3 + H_2O$
$3NiO_4^{-2} + 4Fe + 6H^+ \rightarrow 3NiO + 2Fe_2O_3 + 3H_2O$
Oxyanions of transition metals of the fifth period
$HZrO_3^- + H^+ \rightarrow ZrO_2 + H_2O$
$6NbO_3^- + 2Fe + 6H^+ \rightarrow 6NbO_2 + Fe_2O_3 + 3H_2O$
$2NbO_3^- + 2H^+ \rightarrow Nb_2O_5 + H_2O$
$3MoO_4^{-2} + 2Fe + 6H^+ \rightarrow 3MoO_2 + Fe_2O_3 + 3H_2O$
$2TcO_4^- + 2Fe + 2H^+ \rightarrow 2TcO_2 + Fe_2O_3 + H_2O$
$2RuO_4^{-2} + 2Fe + 4H^+ \rightarrow Ru_2O_3 + Fe_2O_3 + 2H_2O$
$2RuO_4^- + 2Fe + 2H^+ \rightarrow 2RuO_2 + Fe_2O_3 + H_2O$
$2RhO_4^{-2} + 2Fe + 4H^+ \rightarrow Rh_2O_3 + Fe_2O_3 + 2H_2O$
Oxyanions of transition metals of the sixth period
$HfO_3^{-2} + 2H^+ \rightarrow HfO_2 + H_2O$
$2TaO_3^- + 2H^+ \rightarrow Ta_2O_5 + H_2O$
$3WO_4^{-2} + 2Fe + 6H^+ \rightarrow 3WO_2 + Fe_2O_3 + 3H_2O$
$6WO_4^{-2} + 2Fe + 12H^+ \rightarrow 3W_2O_5 + Fe_2O_3 + 6H_2O$
$2ReO_4^- + 2Fe + 2H^+ \rightarrow 2ReO_2 + Fe_2O_3 + H_2O$
$3ReO_4^{-2} + 2Fe + 6H^+ \rightarrow 3ReO_2 + Fe_2O_3 + 3H_2O$
$3OsO_4^{-2} + 2Fe + 6H^+ \rightarrow 3OsO_2 + Fe_2O_3 + 3H_2O$
$3IrO_4^{-2} + 2Fe + 6H^+ \rightarrow 3IrO_2 + Fe_2O_3 + 3H_2O$

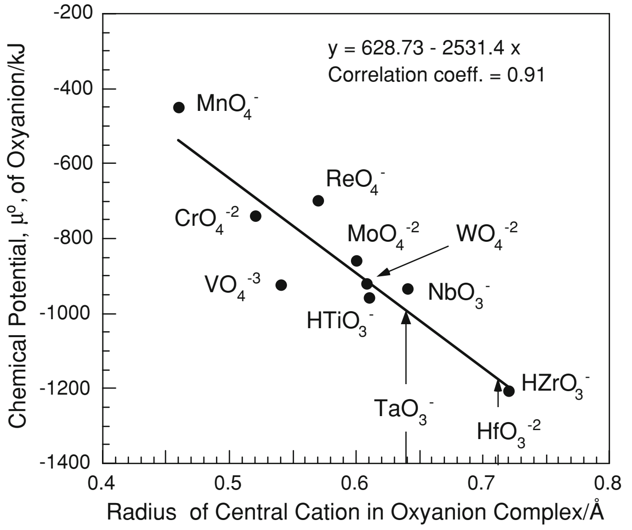

Fig. 5 Estimation of the chemical potentials, μ^o, for TaO_3^- and HfO_3^- anions

and $\mu^o(TaO_3^-) = -990$ kJ mole^{-1}. Ionic radii used in this approach were taken from Shannon and Prewitt [27, 28] or from Pauling [29].

It should be noted that in some cases, the formation of the metal oxide from the oxyanion of the transition metal does not involve a reduction reaction but rather a chemical (non-electrochemical) reaction. An example is:

$$HZrO_3^- + H^+ \rightarrow ZrO_2 + H_2O. \quad (6)$$

Thus the oxyanion can form its transition metal oxide without the participation of the underlying iron substrate in an electrochemical reaction.

Other instances considered here of chemical (i.e., non-electrochemical) reactions to form the metal oxide of the oxyanion are the reaction of $HTiO_3^-$ to TiO_2, of NbO_3^- to Nb_2O_5, of HfO_3^{-2} to HfO_2, and of TaO_3^- to Ta_2O_5.

Table 3 shows the calculated standard free energies ΔG^o for the formation of transition metal oxides from their oxyanions. These values of ΔG^o per mole of oxyanion are plotted in Fig. 6, as a function of the atomic number of the central atom in the oxyanion. Values of ΔG^o per mole of oxyanion decrease with atomic number within a given period in the periodic table. Moreover, values of ΔG^o per mole of oxyanion are periodic in the sense that this pattern is repeated for the fourth through sixth periods of the periodic table.

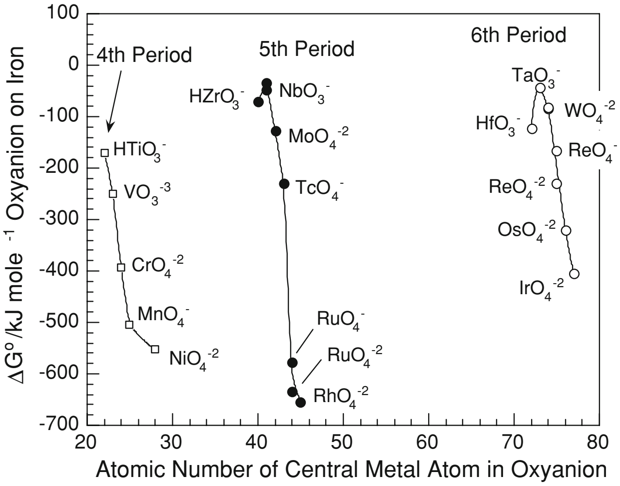

Fig. 6 Calculated standard free energy change ΔG^o for the reaction of various oxyanions with iron surfaces

Figure 6 shows that surface treatment of iron (steel) with any of the oxyanions considered here under standard conditions leads to a spontaneous reaction, as evidenced by negative values of ΔG^o. The oxyanions which produce more negative values of ΔG^o (per mole of oxyanion) than that of CrO_4^{-2} are MnO_4^-, NiO_4^{-2}, RuO_4^-, RuO_4^{-2}, and RhO_4^{-2}.

Table 3 Calculated results for the free energy change ΔG^o for the reduction of transition metal oxyanions on an iron surface

Metal atom	Atomic number	Oxyanion	Resulting oxide	ΔG^o (reaction) in kJ	Number of oxyanions in overall reaction	ΔG^o/oxyanion in kJ mole^{-1}
Ti	22	$HTiO_3^-$	TiO_2	−170	1	−170
V	23	VO_4^{-3}	V_2O_3	−1492	6	−249
Cr	24	CrO_4^{-2}	Cr_2O_3	−788	2	−394
Mn	25	MnO_4^-	MnO_2	−1,009	2	−505
Ni	28	NiO_4^{-2}	NiO	−1,659	3	−553
Zr	40	$HZrO_3^-$	ZrO_2	−70	1	−70
Nb	41	NbO_3^-	NbO_2	−278	6	−47
			Nb_2O_5	−69	2	−35
Mo	42	MoO_4^{-2}	MoO_2	−380	3	−127
Tc	43	TcO_4^-	TcO_2	−457	2	−229
Ru	44	RuO_4^{-2}	Ru_2O_3	−1,268	2	−634
		RuO_4^-	RuO_2	−1,154	2	−577
Rh	45	RhO_4^{-2}	Rh_2O_3	−1,310	2	−655
Hf	72	HfO_3^{-2}	HfO_2	−123	1	−123
Ta	73	TaO_3^-	Ta_2O_5	−83	2	−42
W	74	WO_4^{-2}	WO_2	−253	3	−84
			W_2O_5	−493	6	−82
Re	75	ReO_4^-	ReO_2	−332	2	−166
		ReO_4^{-2}	ReO_2	−686	3	−229
Os	76	OsO_4^-	OsO_2	−960	3	−320
Ir	77	IrO_4^{-2}	IrO_2	−1,214	3	−405

The oxyanions which produce values of ΔG^{o} (per mole of oxyanion) similar to CrO_4^{-2} are OsO_4^{-2}, and IrO_4^{-2}.

The other oxyanions considered here produce values of ΔG^{o} (per mole of oxyanion) which are less negative than that of CrO_4^{-2}. These oxyanions are $HTiO_3^{-}$, VO_4^{-3}, $HZrO_3^{-}$, NbO_3^{-}, MoO_4^{-2}, TcO_4^{-}, HfO_3^{-2}, TaO_3^{-}, WO_4^{-2}, ReO_4^{-}, and ReO_4^{-2}.

2.3 Non-standard conditions

For aqueous electrochemistry, standard conditions (which refer to ΔG^{o}) are unit activity for all dissolved ions (and 298°K). This includes the hydrogen ion H^{+}, so that $pH = 0$ is the pH in the standard state.

The free energy change ΔG for non-standard conditions is related to the free energy change ΔG^{o} in the standard state by:

$$\Delta G = \Delta G^{o} + 2.303\ RT \log K_{eq} \qquad (7)$$

where K_{eq} is the equilibrium constant for the reaction as written. For example, for the reaction of molybdates with iron:

$$2Fe + 3MoO_4^{-2} + 6H^{+} \rightarrow Fe_2O_3 + 3MoO_2 + 3H_2O \qquad (3)$$

$$K_{eq} = \frac{1}{\left[MoO_4^{-2}\right]^3\left[H^{+}\right]^6}. \qquad (8)$$

Use of Eq. 8 in 7 gives:

$$\Delta G = -380.1 - 17.118 \log\left[MoO_4^{-2}\right] + 34.276\ pH \qquad (9)$$

where all free energy values are in kJ. Figure 7 shows how the free energy change ΔG varies with the concentration of molybdate ion (MoO_4^{-2}) and with the pH according to Eq. 9. The free energy change becomes more negative with increasing concentration of MoO_4^{-2} (at fixed pH) and with decreasing pH (at fixed MoO_4^{-2} concentration).

Note from Fig. 7 that Eq. 9 proceeds spontaneously at pH 7 and pH 0, but not at pH 14. The borderline between regions of spontaneity and non-spontaneity can be determined by setting $\Delta G = 0$ in Eq. 9 and solving for pH. The result is:

$$pH = 11.102 + 0.5 \log\left[MoO_4^{-2}\right]. \qquad (10)$$

This straight line is shown in Fig. 8.

The corresponding values of electrode potential E for the reaction in Eq. 3 are also given in Fig. 7. These values of E are given by $\Delta G = -nFE$, where all terms have their usual meaning.

Calculations for the change in free energy were also performed for the case in which the formation of the metal oxide from the oxyanion of the transition metal does not involve a reduction reaction but rather a chemical (non-electrochemical) reaction. For the zirconate ion on iron, mentioned earlier, results are shown in Fig. 9. Again, the free energy change becomes more negative with increasing concentration of oxyanion (at fixed pH) and with decreasing pH (at fixed oxyanion concentration). Note from Fig. 9 that Eq. 6 proceeds spontaneously at pH 7 and pH 0, but not at pH 14.

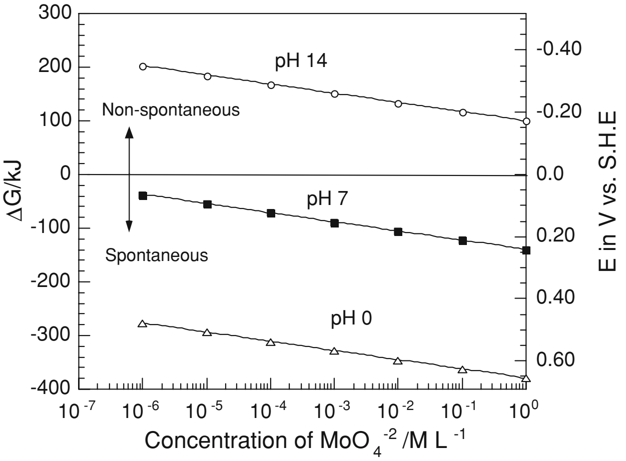

Fig. 7 Calculated free energy change ΔG at various oxyanion concentrations and pH values for the reaction of molybdate ions (MoO_4^{-2}) with iron surfaces

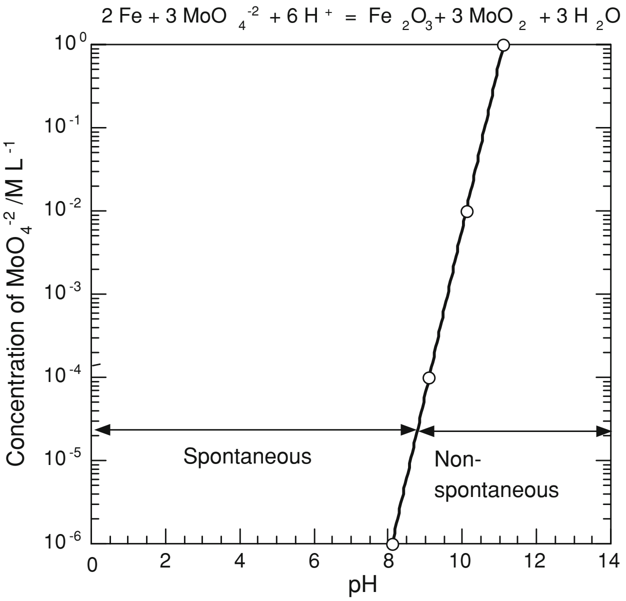

Fig. 8 Regions of spontaneity and non-spontaneity for the reaction of molybdate ions with an iron surface

Regions of spontaneity (for iron) are shown in Figs. 10, 11, and 12 for oxyanions of metals in the fourth through sixth periods of the periodic table.

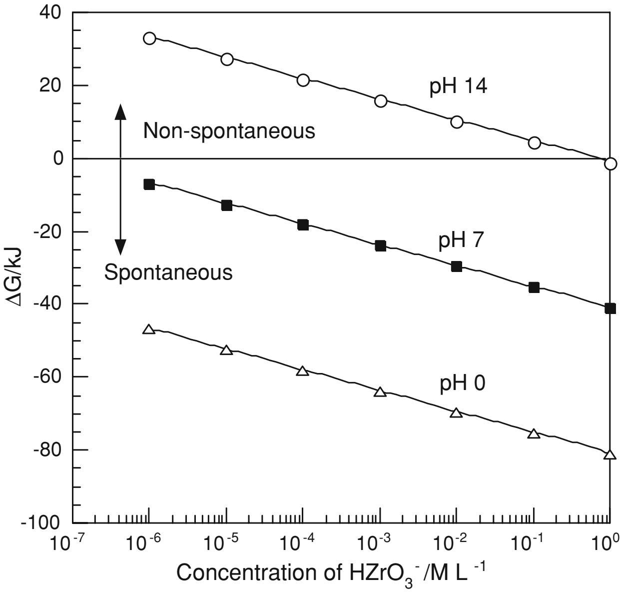

Fig. 9 Calculated free energy change ΔG at various oxyanion concentrations and pH values for the reaction of zirconate ions ($HZrO_3^-$) with iron surfaces

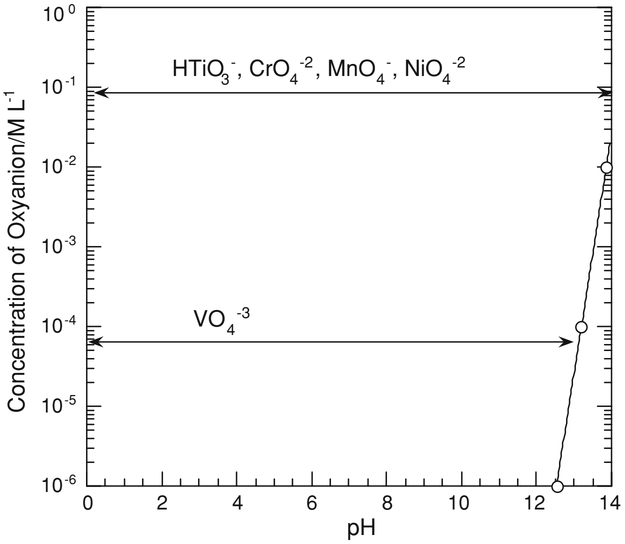

Fig. 10 Regions of spontaneity for the reaction of iron with oxyanions of the fourth period of the periodic table

2.4 The case for aluminum

If the substrate metal is aluminum rather than iron, the overall reactions are similar. For molybdates, for example, Eq. 3 is replaced by:

$$2Al + 3MoO_4^{-2} + 6H^+ \rightarrow Al_2O_3 + 3MoO_2 + 3H_2O. \quad (11)$$

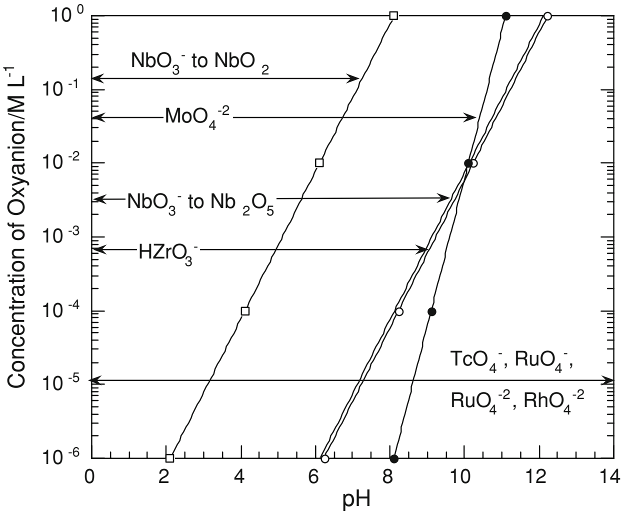

Fig. 11 Regions of spontaneity for the reaction of iron with oxyanions of the fifth period of the periodic table

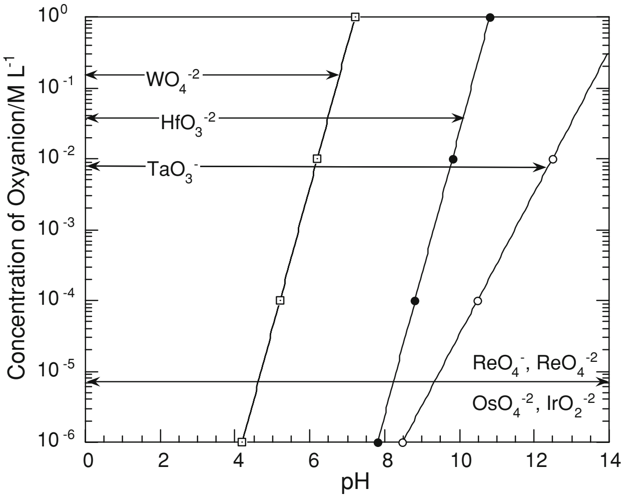

Fig. 12 Regions of spontaneity for the reaction of iron with oxyanions of the sixth period of the periodic table

Values of ΔG^o for the case of aluminum are considerably more negative than for iron because the chemical potential $\mu^o(Al_2O_3)$ is more negative than that for $\mu^o(Fe_2O_3)$. These values are −1,576 and −740 kJ mole^{-1}, respectively [16].

All the corresponding electrochemical reactions on aluminum given in Table 2 are spontaneous over the entire pH range of 0 to 14. On aluminum, the chemical (i.e., non-electrochemical reactions have the same regions of stability as for iron and have been given in Figs. 8, 10, and 11.

2.5 Limitations

These calculations carry with them all the usual limitations of thermodynamics. That is, thermodynamics is the realm of what is possible, but gives no information on the rates of reactions. Moreover, the actual corrosion properties of the resulting oxides on iron or aluminum must be determined by experimental measures.

3 Conclusions

Thermodynamic calculations have been made for the oxyanions of transition metals in regard to replacing chromate as a corrosion inhibitor or surface treatment agent.

The oxyanions considered here are titanate ($HTiO_3^-$), vanadate (VO_4^{-3}), chromate (CrO_4^{-2}), permanganate (MnO_4^-), nickelate (NiO_4^{-2}), zirconate ($HZrO_3^-$), niobate (NbO_3^-), molybdate (MoO_4^{-2}), pertechtate (TcO_4^-), ruthenate (RuO_4^{-2} and RuO_4^-), rhodate (RhO_4^{-2}), hafnate (HfO_3^{-2}), tantalate (TaO_3^-), tungstate (WO_4^{-2}), rhenate (ReO_4^{-2} and ReO_4^-), osmate (OsO_4^{-2}), and iridate (IrO_4^{-2}).

In most of the reactions involving transition metal oxyanions, the oxide of the transition metal is formed by electrochemical reduction of the oxyanion. A chemical (i.e., non-electrochemical) reaction is involved in the formation of TiO_2 from $HTiO_3^-$, ZrO_2 from $HZrO_3^-$, Nb_2O_5 from NbO_3^-, HfO_2 from HfO_3^{-2}, and Ta_2O_5 from TaO_3^-.

All reactions with iron or aluminum are spontaneous over a wide range of oxyanion concentrations and pH. Values of the free energy change, ΔG^o per mole of oxyanion, decrease with atomic number of the central metal atom within a given period in the periodic table. Moreover, values of ΔG^o per mole of oxyanion are periodic in that this pattern is repeated for the fourth through sixth periods of the periodic table.

For iron, the oxyanions which produce more negative values of ΔG^o (per mole of oxyanion) than that of CrO_4^{-2} are MnO_4^-, NiO_4^{-2}, RuO_4^-, RuO_4^{-2}, and RhO_4^{-2}.

For iron, the oxyanions which produce values of ΔG^o (per mole of oxyanion) similar to CrO_4^{-2} are OsO_4^{-2}, and IrO_4^{-2}.

For iron, the other oxyanions considered here produce values of ΔG^o (per mole of oxyanion) which are less negative than that of CrO_4^{-2}. These oxyanions are $HTiO_3^-$, VO_4^{-3}, $HZrO_3^-$, NbO_3^-, MoO_4^{-2}, TcO_4^-, HfO_3^{-2}, TaO_3^-, WO_4^{-2}, ReO_4^-, and ReO_4^{-2}.

This thermodynamic approach gives no information on the rates of reactions. Moreover, the actual corrosion properties of the resulting oxides on iron or aluminum must be determined by experimental measures.

References

1. Kendig MW, Buchheit RG (2003) Corrosion 59:379
2. O'Brien P, Kortenkamp A (1995) Trans Met Chem 20:636
3. Chambers BD, Taylor SR, Kendig MW (2005) Corrosion 61(5):480–489
4. Silva JWJ, Codaro EN, Nakazato RZ, Hein LRO (2005) Appl Surf Sci 252:1117
5. Magalhaes AAO, Margarit ICP, Mattos OR (2004) J Electroanal Chem 572:433
6. El Abedin SZ (2001) J Appl Electrochem 31:711
7. Breslin CB, Treacy G, Carroll WM (1994) Corros Sci 36(7):1143
8. Guan H, Buchheit RG (2004) Corrosion 60(3):284–296
9. Hughes AE, Gorman JD, Harvey TG, Galassi A, McAdam G (2006) Corrosion 62:773
10. Hinton BRW, Arnott DR, Ryan NE (1986) Mater Forum 9:162
11. Vetere VF, Romagnoli R (1994) Br Corros J 29:115
12. Leggat RB, Zhang W, Buchheit RG, Taylor SR (2002) Corrosion 58:322
13. Sinko J (2001) Prog Org Coat 42:267
14. Yao K, Song S, Shen N (1991) Mater Chem Phys 28:303
15. Sugerman G, Monte SJ (1988) Mod Paint Coat 78(6):50
16. Pourbaix M (1966) Atlas of electrochemical equilibria. Pergamon Press, Oxford
17. McCafferty E, Wightman JP (1998) Surf Interface Anal. 26:549
18. Halada GP, Clayton CR, Herman H, Sampath S, Tiwari R (1995) J Electrochem Soc 142:74
19. Li X-Y, Akiyama E, Habazaki H, Kawashima A, Asami K, Hashimoto K (1998) Corros Sci 40:821
20. Kim JH, Akiyama E, Habazaki H, Kawashima A, Asami K, Hashimoto K (1994) Corros Sci 36:511
21. Bhattarai J, Akiyama E, Kawashima A, Asami K, Hashimoto K (1995) Corros Sci 37:2071
22. Li X-Y, Akiyama E, Habazaki H, Kawashima A, Asami K, Hashimoto K (1997) Corros Sci 39:1365
23. Asami K, Chen S-C, Habazaki H, Hashimoto K (1993) Corros Sci 35:43
24. Hoppe H-W, Strehblow H-H (1990) Surf Interface Anal 16:271
25. Patrito EM, Torresi RM, Leiva EPM, Macagno VA (1992) Electrochim Acta 37:281
26. Bard AJ, Parsons R, Jordan J (eds) (1985) Standard electrode potentials in aqueous solution. Marcel Dekker, Inc., New York
27. Shannon RD, Prewitt CT (1970) Acta Crystallogr B26:1046
28. Shannon RD, Prewitt CT (1969) Acta Crystallogr B25:925
29. Pauling L (1948) The nature of the chemical bond. Cornell University Press, Ithaca, p 343